

# Acidity of all-silica MCM-41—studied by laser spectroscopy of adsorbed fluorescent probe compounds

Ali A. El-Rayyes, Abdulrahman A. Al-Arfaj, Uwe K. A. Klein, and Sami A. I. Barri\*

*Chemistry Department, King Fahd University of Petroleum and Minerals, Dhahran 31261, Saudi Arabia*

Received 3 April 2004; accepted 8 June 2004

The polarity within the channel environment of all-silica MCM-41 and the surface acidity were probed by the adsorption of rhodamine-B lactone (RhB-L) and 1-naphthylamine (NA) respectively. The photochemical properties of these probe compounds were studied by laser-induced fluorescence spectroscopy and compared with their properties in solution. The environment within the channels was found to be as polar as methanol. The fluorescence wavelength and decay rate have shown that when adsorbed on all-silica MCM-41, the lactone ring in RhB-L was opened to form the zwitterion (RhB-Z). It was not possible to assess whether RhB-L was protonated by the surface of MCM-41 because the fluorescence of both the RhB-Z and the cationic form RhB-C are almost identical. NA was protonated at the ground state on the surface of all-silica MCM-41. The proton, however, was donated back to the surface upon excitation with laser. From the  $pK_a$  of the conjugate acid of NA and the fluorescence decay time of the excited state of NA (NA\*), the acidity of the surface of the all-silica MCM-41 was estimated to be equivalent to an aqueous perchloric acid with pH 1.8–2.5, depending on the level of loading of NA. The origin of the acid surface was concluded to be the silanol groups known to be present on the surface. The nature of these groups and the influence of the polarity and the solvation effect of the framework on the acidity were discussed.

**KEY WORDS:** All-silica MCM-41; fluorescent probe compounds; RhB-2.

## 1. Introduction

The internal surface of MCM-41 type materials is known to contain silanol groups as evidenced by solid state nuclear magnetic resonance spectroscopy [1–3]. In a previous paper it was shown that the all-silica composition of MCM-41 was catalytically active for the cracking of polymers and there was strong evidence that the catalytic reaction occurred over weak acid sites present within the channels [4]. The silanol groups were most probably the centres of these acid sites. This paper reports on research work undertaken to characterise the polarity of the environment within the channels and the strength of the acid sites present on its surface by studying the photochemical properties of probe molecules adsorbed within the pores of MCM-41.

The photochemical properties of probe molecules have been studied before on the surfaces of solid catalysts such as silica, alumina, metal oxides and zeolites or in solution [5–24]. For example, the fluorescence behaviour of Rodamine-B (RhB) has shown a transition from the zwitterion form (RhB-Z) to the lactone form (RhB-L) upon encapsulation in  $SiO_2$  from solution, and transition to the cationic form (RhB-C) upon encapsulation in Si–Ti binary oxides [16]. A key to the interpretation of the results is the properties of these

probe molecules in solutions. The polarity of the solution has been reported to affect the photochemical and photophysical properties of RhB. The RhB-Z form dominates the equilibrium with the RhB-L form in protic solvents, whereas the RhB-C form is present in acidic solutions [17–20]. The RhB-Z and RhB-C forms have similar absorption and fluorescence bands except for a small shift in the fluorescence spectra of the former towards longer wavelengths. On the other hand, the RhB-L form has only weak absorption and fluorescence bands and is colourless [16].

The surface acidity of solids, such as zeolite Y, can be probed by the adsorption of 1-naphthylamine (NA), and the proton exchange can be studied by laser-induced fluorescence spectroscopy [25]. Again the properties of NA in solution strengthened the interpretation of the findings of NA adsorbed in zeolite Y [26]. The photochemical and photophysical properties of NA were studied in perchloric acid solutions of varying concentrations and correlated with the fluorescence characteristics of the chromophore when adsorbed in zeolite Y with varying acidities. The excited state of the protonated NA adsorbed on the solid Bronsted acid may fluoresce and return to the ground state if the solid is of high acid strength. On the other hand, it may donate the proton back to the conjugate base on the solid surface if the acid strength is relatively low. In addition the lifetime of the fluorescing species may be correlated with the strength of interaction with the solid host.

The polarity within the channel environment of MCM-41 and the surface acidity were probed by

\*To whom correspondence should be addressed.

Current address: Davy-Faraday Research Laboratory, The Royal Institution of Great Britain, 21 Albemarle Street, London WC1.  
E-mail: sami@ri.ac.uk

adsorbing RhB-L and NA, respectively. The photochemical and photophysical properties of these fluorophores were studied by laser-induced fluorescence spectroscopy and compared with the corresponding characteristics of the same molecules in solution.

## 2. Experimental

### 2.1. Materials and characterisation

Rhodamine B HCl, Fluka, salt was used as received without further purification. Rhodamine B Lactone was obtained from aqueous Rhodamine B solution according to the reported procedure [17]. NA was supplied by Fluka company and was used after recrystallisation from petroleum ether followed by sublimation. All the solvents used in this work were of spectral grade and were dried over molecular sieves 5A prior to use. Polydimethylsiloxane (PDMS), a two-component polymer: RTV 615A and RTV 615B, was provided by General Electric Silicones. MCM-41 (KT-1 and KTM-3) materials were synthesized and characterised by X-ray powder diffraction and benzene adsorption as previously described [27]. The MCM-41 samples were chemically analysed for aluminium and other elements. The impurity level was lower than 10 ppm, as determined by ICP-AIS.

### 2.2. Preparation of solid-organic probe complex and the PDMS membrane

RhB-L was dissolved in cyclohexane and solutions with increasing dilutions were prepared. The solutions were used to prepare samples with increasing amounts of RhB-L adsorbed on MCM-41. Samples of MCM-41 were dried at 500 °C over night and transferred, after cooling in a desiccator under vacuum, into a solution of the fluorophore. Aliquots of the dried MCM-41 (150 mg) were contacted with 5.0 ml of RhB-L/cyclohexane solutions of the following concentrations:  $2.26 \times 10^{-5}$  M,  $2.26 \times 10^{-4}$  M,  $4.50 \times 10^{-3}$  M, and  $1.35 \times 10^{-2}$  M. The suspensions were stirred for about 15 h to reach adsorption equilibrium. The complex was then collected by filtration, washed three times with the solvent to remove the externally adsorbed molecules, and then dried on a vacuum line. The same procedure was followed for the adsorption of NA on MCM-41 except that n-hexane solvent was used and the concentrations of the solutions were  $1.30 \times 10^{-4}$  M,  $1.10 \times 10^{-3}$  M,  $9.75 \times 10^{-3}$  M, and  $1.83 \times 10^{-2}$  M.

The percentage loading of the fluorophore on the molecular sieves was calculated by comparing the UV spectra of the original solution to that of the filtrate. In all the preparations there was a change in the colour of the formed complex indicating interactions with acidic sites.

In a typical preparation of a MCM-41 PDMS film, 1 g of n-hexane and 30–70 mg of the MCM-41 included

probe molecule and dried thoroughly under vacuum was sonicated for a period of 1 h to break the aggregates. Then 1 g of RTV 615 A was added and the mixture was sonicated again for a period of 6 h. Finally 100 mg of RTV 615 B was added and the mixture was further sonicated for 20 min. The mixture was cast onto a glass plate and heated at 60 °C overnight. The membrane was removed from the glass and was further dried in the oven.

### 2.3. Absorption and fluorescence spectra

Steady-state UV–Vis absorption measurements for solutions are obtained using  $\lambda$ -5 (Perkin-Elmer) Spectrophotometer. Fluorescence spectra for the solutions and the MCM-41 films were recorded with an SPF-500 spectrofluorometer from SLM Instruments. The fluorescence spectra were corrected for the intensity of the lamp and the sensitivity of the photomultiplier tube. The fluorescence decay time measurements were recorded on a mode-locked Nd: YAG laser (Spectra-Physics model 3800) with a mode locker (Spectra-Physics model 451) operating at 82 MHz repetition. Cavity dumping at 4 MHz was performed. The output pulses were frequency doubled (Spectra-Physics model 390 frequency doubler). The excitation wavelength was chosen appropriately and the fluorescence decay signals of the probe molecule were collected at the wavelength of maximum fluorescence emission. Lifetimes were measured using the Applied Photophysics photon-counting spectrometer system, model PS 60, equipped with a XP 2020Q photomultiplier. The actual pulse width of the excitation pulse is less than 10 ps however, due to the response time of the photon counting system it is broadened to 350 ps. Data were collected through a multichannel analyzer and then transferred to a computer for analysis.

Solutions of the probe molecules in different solvents were kept at ( $1 \times 10^{-5}$  M) for the absorption and emission measurements. But solutions with varying concentrations were also prepared when needed to study the effect of varying concentrations.

## 3. Results and discussion

### 3.1. Properties of MCM-41 samples

The properties of the MCM-41 samples used in this study are given in table 1. Characterisation by X-ray diffraction and benzene adsorption has shown high crystallinity for both samples.

X-ray diffraction has shown the materials to have typical patterns of the hexagonal phase that characterises the MCM-41 structure. The material crystallised using conventional oven (KT-1) had  $d_{100}$  at a lower  $2\theta$  angle than the sample crystallised using microwave heating (KTM-3) due to a larger unit cell parameters and pore diameter.

Table 1  
Properties of MCM-41 samples synthesised

Sample code	Heating mode	Crystallisation time (h)	$d_{100}$ (Å)	$a_0$ (Å)	$V_p$ (cc/g)	$P/P_0$ (capillary condensation)	$d_p$ (Å)	$\delta$ (Å)
KT-1	Conventional	96	53.5	61.8	0.74	0.36	50.9	10.9
KTM-3	Microwave	5.0	38.6	44.6	0.73	0.19	36.6	8.0

Note:  $d_p$  is the pore diameter and  $\delta$  is the wall thickness.

The X-ray diffraction results were well supported by the benzene adsorption measurements. The adsorption capacity ( $V_p$ ) of both samples were comparable and the highest as function of time of crystallisation. The pore diameter ( $d_p$ ) and the wall thickness ( $\delta$ ) were calculated from the measurements of the adsorption capacity, the wall density by benzene displacement at room temperature, and the unit cell parameter as described elsewhere [27]. As seen in table 1, KTM-3 has a smaller pore diameter and wall thickness than KT-1. A possible reason for the shrinkage in the KTM-3 sample relative to the KT-1 sample is smaller hydration shells around the micelle templates upon the application of microwave energy. The reason for the choice of these samples was their reported catalytic activity for polyethylene cracking and the effect of the pore diameter on the level of the activity [4].

### 3.2. Polarity characterisation

#### 3.2.1. RhB fluorescence in homogeneous solution

The change in the fluorescence  $\lambda_{\max}$  and the corresponding fluorescence lifetime upon changing the solvent polarity is shown in table 2. The spectra of RhB-L in the various solvents agreed well with the already published spectra [17]. In non-polar solvents ( $\epsilon \leq 15$ ), the solutions were colourless indicating the predominance of the RhB-L form in the ground state, while in

polar solvents ( $\epsilon > 15$ ), the solutions were red indicating the opening of the lactone ring and the formation of the quinoid (cationic) RhB-C form in the ground state. Excitation of a dilute solution of RhB-L ( $1.0 \times 10^{-5}$  M) led to a blue-violet fluorescence in non-polar solvents (benzene and cyclohexane) and to an orange fluorescence in polar solvents (methanol and DMSO). There was a red shift in the  $\lambda_{\max}$  of the fluorescence on changing from non-polar to polar solvents and the fluorescence quantum yield increased till it reached a maximum in methylene chloride and 1,4 dioxane, then it decreased by further increasing the polarity (acetonitrile > methanol > DMSO) as shown in table 2. In highly polar media the equilibrium,  $\text{RhB-L} \rightleftharpoons \text{RhB-Z}$ , was completely shifted to the right. The fluorescence decay time measurements generally showed a long decaying component in non-polar solvents and a short decaying species in polar media. These corresponded to the lactone form and the zwitterion form, respectively. The increase in the fluorescence lifetime of the RhB-L appeared to be more smoothly correlated with the shift in  $\lambda_{\max}$  as shown in figure 1. Upon the increase in the solvent polarity and the conversion to the RhB-Z, there was a large and sharp increase in the  $\lambda_{\max}$ . The transformation was also associated with a sharp decrease in the fluorescence lifetime in the solvents acetonitrile, methanol, water or dimethylsulfoxide. The effect of the RhB-L concentration in methanol solution

Table 2  
Fluorescence  $\lambda_{\max}$  (nm) and fluorescence decay time  $\tau$  (ns) for rhodamine B (RhB) in solvents with different dielectric constants

Solvent	$\epsilon^b$	RBL fluorescence	
		$\lambda_{\max}$ (nm)	$\tau$ (ns)
Cyclohexane	2.02	375	1.60
1,4-dioxane	2.20	460	13.8
Benzene	2.30	450	7.72
n-dibutylether	3.00	420	4.73
Chlorobenzene	5.70	460	11.9
Dichloromethane	9.10	570	3.00
Ethanol	25.1	580	1.50
Methanol	33.6	590	2.85
Acetonitrile	36.8	570	1.93
Dimethylsulfoxide	46.5	605	2.40
Water	80.0	580	1.50

Note:  $\lambda$  excitation = 300 nm.

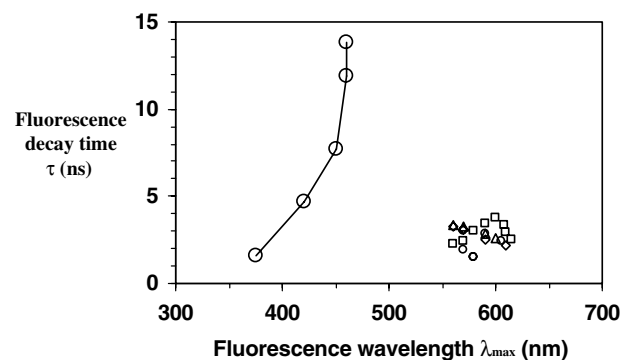


Figure 1. Fluorescence decay times as a function of fluorescence wavelengths; (○) RhB in solutions with different polarities; (□) RhB in methanol in varying concentrations; (◇) RhB in MCM-41 (KTM-3) in varying loading; (△) RhB in MCM-41 (KT-1) in varying loading.

Table 3

Fluorescence  $\lambda_{\text{max}}$  (nm) and fluorescence decay time  $\tau$  (ns) for rhodamine B (RhB) in methanol solution at different concentrations

Concentration	Fluorescence $\lambda_{\text{max}}$ (nm)	Fluorescence decay time $\tau$ (ns)
$3.5 \times 10^{-6}$	560	2.2
$1.75 \times 10^{-5}$	570	2.4
$8.75 \times 10^{-5}$	580	3.0
$4.38 \times 10^{-4}$	590	3.4
$2.19 \times 10^{-3}$	600	3.8
$4.38 \times 10^{-3}$	608	3.3
$6.56 \times 10^{-3}$	610	2.9
$1.10 \times 10^{-2}$	615	2.6

Note:  $\lambda$  excitation = 300 nm.

on its photochemical behaviour is shown in table 3. As seen, there was a red shift in the fluorescence  $\lambda_{\text{max}}$  and the lifetime increased and then decreased as the RhB-L concentration increased. It appeared that the trend in the lifetime was a product of a quenching effect reducing the lifetime and a bi-molecular interaction at high RhB-L concentration stabilising the excited species.

### 3.2.2. RhB-L adsorbed on MCM-41

The photochemical properties of RhB-L adsorbed in the channels of all-silica MCM-41 have shown the surface to be as polar as alcohols. The first indication of the polarity of the surface was observed when a pink colour appeared upon the adsorption of RhB-L on MCM-41 sample from a cyclohexane solution. The colour intensified into a red colour when the loading increased. Furthermore, the emission spectra of the species adsorbed show a band at  $\lambda_{\text{max}}$  between 560 and 610 nm, indicating the opening of the lactone ring and the presence of the RhB-Z form or even perhaps the RhB-C form in the ground state. table 4 and figure 2, show the fluorescence  $\lambda_{\text{max}}$  and the fluorescence decay time for RhB adsorbed in the meso-pores at different loading levels. In general  $\lambda_{\text{max}}$  of the fluorescence increased on increasing the loading level. The fluorescence  $\lambda_{\text{max}}$  and lifetime found corresponded well to the

Table 4

Fluorescence  $\lambda_{\text{max}}$  (nm) and fluorescence decay time  $\tau$  (ns) for rhodamine B (RhB) adsorbed in the pores of MCM-41 materials

Catalyst	Loading level (mmol/g)	Fluorescence $\lambda_{\text{max}}$ (nm)	Fluorescence decay time $\tau$ (ns)
KTM-3	$2.9 \times 10^{-1}$	610	2.2
	$1.5 \times 10^{-1}$	590	2.5
	$2.3 \times 10^{-4}$	570	3.1
	$2.3 \times 10^{-5}$	560	3.3
KT-1	$2.9 \times 10^{-1}$	600	2.6
	$1.5 \times 10^{-1}$	590	2.9
	$2.3 \times 10^{-4}$	570	3.2
	$2.3 \times 10^{-5}$	560	3.4

Note:  $\lambda$  excitation = 300 nm.

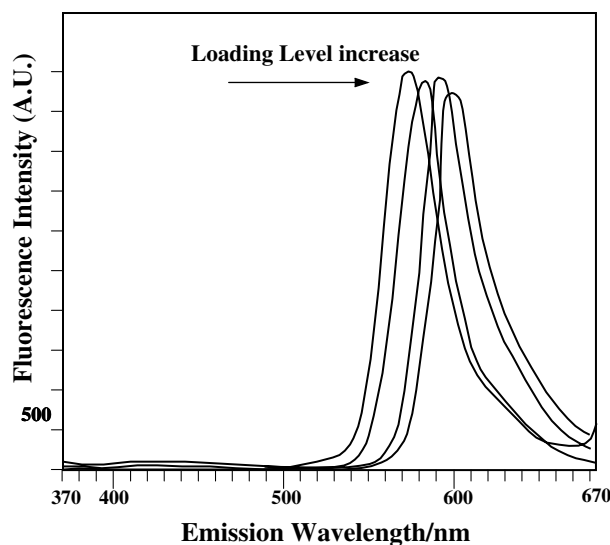


Figure 2. Emission spectra of RhB adsorbed at the surfaces of MCM-41 (KT-1),  $\lambda$  excitation = 300 nm.

values found in solutions with higher polarities than methylene chloride. As seen in figure 1, the values also corresponded with the presence of RhB-Z if not RhB-C. The results suggested a highly polar environment inside the channels, which was comparable to that in solvents with  $\epsilon > 15$ .

The source of the polarity within the channels of the all-silica MCM-41 was most likely to be the hydroxyl groups, which are known to exist lining the wall of the mesoporous pores [1–3]. Polarity in fluids originates from dipoles, which are mobile and change direction, giving a net electric field of zero. Within the pores of MCM-41, however, the dipoles are fixed and there would be a permanent electric field present. This could strongly polarise a molecule present within its environment.

The colour of the complex, the emission wavelength  $\lambda_{\text{max}}$ , and the lifetime of the excited state have all indicated the opening of the lactone ring upon adsorption of RhB-L in the MCM-41 channels. These properties are consistent with the presence of a high polarising environment in the pores. This supported previous work, which showed a high catalytic activity of the all-silica MCM-41 for the cracking of polyethylene [4]. However, the RhB-L probe was not a suitable molecule to ascertain information on the presence of Bronsted acidity, due to the lack of distinction between the presence of the cationic form RhB-C and the zwitterion form RhB-Z.

### 3.3. Acidity characterisation

The acidity of the MCM-41 surface was probed by the adsorption of NA. The surface was found to have relatively weak Bronsted acidity as it protonated NA in the ground state. The surface acidity was equivalent to an acidic solution of pH varying between 2.5 and 1.8.

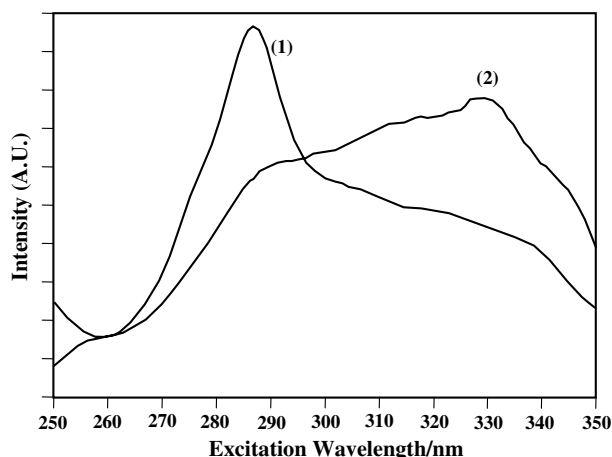


Figure 3. Excitation spectra of NA adsorbed at the surfaces of MCM-41 (KT-1); (1) 0.6 mg NA/g KT-1, (2) 42 mg NA/g KT-1,  $\lambda$  excitation = 300 nm.

The conjugate acid of NA has a  $pK_a$  equal to 3.9, that is in a solution of  $pH \leq 2$ , practically all the NA molecules will be present in the protonated form ( $R-NH_3^+$ ,  $R$  = naphthyl). Excitation spectra of NA adsorbed at the surfaces of the all-silica MCM-41 materials are shown in figure 3. The spectra showed only the absorption of the protonated form at low loading of NA (spectra 1 in the figure), while both the absorption of the neutral and the protonated forms were recorded at high loading level (spectra 2 in the figure). The formation of the  $R-NH_3^+$  was a result of interactions with hydrogen bond donor groups, suggesting the presence of weak Bronsted acid sites on the surface of the catalyst due to the silanol groups.

Emission spectra of both the low and high loaded samples showed fluorescence originating mainly from the neutral form, as shown in figure 4. This meant that  $RNH_3^+$  dissociated in the excited state, and the proton

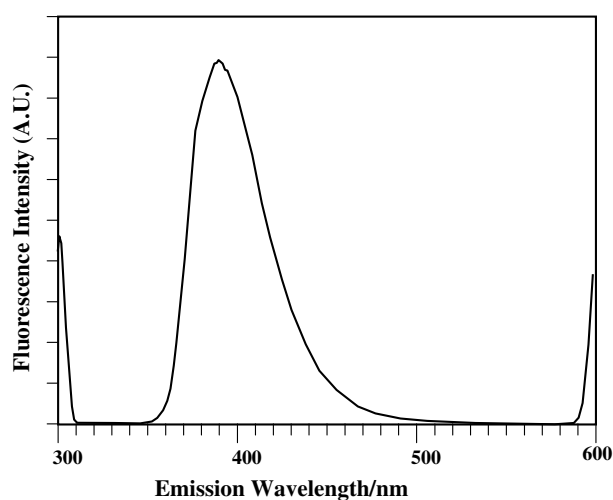
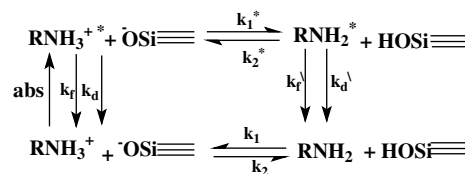


Figure 4. Emission spectra of NA adsorbed at the surfaces of MCM-41 (KT-1),  $\lambda$  excitation = 300 nm and loading =  $2.3 \times 10^{-5}$  mmol/g.



Scheme 1. Proton transfer reaction of  $RNH_2$  at the surface of MCM-41.

returned back to the surface. The excited state proton transfer reaction between  $RNH_3^{+*}$  and the surface silanol groups is presented in scheme 1.

NA was used before to probe the acidity of zeolite Y [25], and in that case, a species X was identified at very high acidity. The fluorescence lifetime of  $X^*$  was found to correlate with the overall acidity of the surface. In the case of MCM-41, however, the acidity was much lower and the species X was absent. As an alternative, the fluorescence lifetime of the excited state of  $NA^*$  was used as an indicator of the acidity of the environment. A correlation between the fluorescence lifetime of  $NA^*$  in perchloric acid solution of varying pH is shown in figure 5. The effect of the pH on the lifetime was most sensitive in the range  $3 > pH > 1$ . The correlation seemed to be affected by other factors too. The polarity of the environment and the solvation effect would be influential factors on the decay rates of  $NA^*$ . In zeolitic materials, and MCM-41 is included, the framework should act like a solvent but not in the same way as in liquid solutions. The rigidity of the framework must contribute negatively to the relaxation of  $NA^*$  and its decay lifetime in comparison with aqueous or methanol solutions, for example. Therefore, one should take into consideration the solvation effect of the framework and the polarity of the environment. The polarity within MCM-41 channels was shown above to be equivalent to that of methanol solvent. It was not possible to measure the lifetime of  $NA^*$  in perchloric acid/methanol solution because of the oxidising properties of perchloric acid.

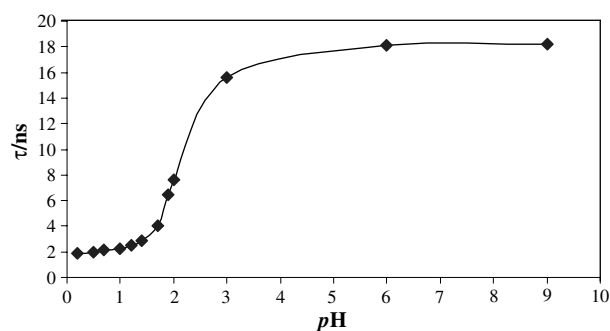


Figure 5. Fluorescence lifetime of  $NA RNH_2^*$  versus the pH of aqueous perchloric acid solution.

Table 5

Absorption and fluorescence  $\lambda_{\max}$  (nm) and fluorescence decay time  $\tau$  (ns) for 1-naphthylamine (NA) adsorbed in the pores of MCM-41 materials

Catalyst	Loading level (mmol/g)	Absorption $\lambda_{\max}$ (nm)	Fluorescence $\lambda_{\max}$ (nm)	Fluorescence decay time $\tau$ (ns)	Estimated pH
KTM-3	$5.5 \times 10^{-1}$	287, 332	378	10.5	2.5
	$2.9 \times 10^{-1}$	287, 332	378	9.6	2.2
	$3.2 \times 10^{-2}$	287	378	8.8	1.9
	$4.2 \times 10^{-3}$	287	378	8.4	1.8
KT-1	$5.5 \times 10^{-1}$	285, 330	380	10.6	2.5
	$2.9 \times 10^{-1}$	285, 330	380	10.5	2.5
	$3.2 \times 10^{-2}$	285	380	10.0	2.3
	$4.2 \times 10^{-3}$	285	380	8.6	1.8

Note:  $\lambda$  excitation = 300 nm.

However, correlation with aqueous solutions has shown useful comparisons.

The fluorescence  $\lambda_{\max}$  of NA\* at the surface was found to be around 380 nm, which was blue shifted with respect to that in aqueous solution. This blue shift may be accounted for by an emission from the un-relaxed excited state of NA\*, which may be a result of interactions with the rigid environment inside the channels and its acidic surfaces. The fluorescence decay lifetimes for NA\* adsorbed at the MCM-41 surfaces were found to be of single exponential with  $\tau$  (NA\*) varying with the loading level of the probe (NA), as shown in table 5. The decay rate of NA\* in MCM-41 materials was found to be between  $9.4 \times 10^7 \text{ s}^{-1}$  and  $1.2 \times 10^8 \text{ s}^{-1}$  depending on the loading level, which was slower than the value of  $1.2 \times 10^8 \text{ s}^{-1}$  found for Y zeolite [25]. The close proximity of the two ranges of decay rate in zeolite Y and MCM-41 did not reflect the large difference in their acidity ranges. Acidity may have had an influence on the decay rate of NA\*, but the solvation effect must also be taken into consideration as discussed above. Zeolite Y channels are of molecular dimension and much narrower than those present in MCM-41. NA\* in the pores of zeolite Y would be expected to be more effectively solvated as the channel wall would be surrounding the probe molecule. The MCM-41 samples used in this study have channel diameters of 36.6 and 50.9 Å. Both materials would not be expected to provide the same environment as those present in zeolite Y, irrespective of the compositions.

These decay rate values for both zeolite Y and MCM-41 were fast compared to the corresponding value of  $5.5 \times 10^7 \text{ s}^{-1}$  measured in aqueous perchloric acid solution where solvent relaxation processes played a major role in stabilizing the excited states of NA\* [26].

By substituting the lifetime values obtained for NA\* in MCM-41 to the curve fitting equation of figure 5, the relative acidity of the environment inside the channels could be estimated. This gave pH values varying between 2.5 and 1.8, as shown in table 5. Fortunately, this range was within the most sensitive range of  $3 > \text{pH} 1$ ; however, the solvation effect would have an

influence too, as discussed above, and it could not be readily measured.

The results presented above clearly showed that the silanol groups present on the surface of the MCM-41 are acidic and capable of protonating NA. NMR has shown that the silanol groups  $\equiv\text{Si}-\text{OH}$  are in different environment as they may be attached to three other silicons *via* oxygen bridges ( $\equiv\text{Si}-\text{O}$ )<sub>3</sub>SiOH (Q3), attached to two other silicon *via* oxygen and another silanol group ( $\equiv\text{Si}-\text{O}$ )<sub>2</sub>Si(OH)<sub>2</sub> (Q2), or attached to another silicon *via* oxygen and two other silanol groups ( $\equiv\text{Si}-\text{O}$ )Si(OH)<sub>3</sub> (Q1). If one considers the possibility of geminal and vincinal silanol groups also, it is likely, therefore, that a distribution of acid sites is present on the surface of the channels. Krasnansky and Thomas reported that silica that has geminal silanol groups protonated 1-aminopyrene [21]. Dehydroxylation of the silica surface at high temperature resulted in reduction in the surface ability to protonate basic compounds. In the case of the MCM-41, however, the material was calcined at a temperature in excess of 500 °C and dehydroxylation of geminal silanols would also be expected to occur. Therefore, the nature of the acid surface, in this case, may be different from that of amorphous silica. For example a concerted interaction [4] of the adsorbed molecule with the surface and the polarity present in the channels may facilitate the proton transfer reaction. Hair and co-workers [22–24] reported only weak interactions with OH groups on the surface of silica with hydrocarbon adsorbate (such as hexane, benzene and styrene), hydrogen bond interactions with oxygenates (such as water, methanol, dimethylether and acetone), and non-ionic interactions with basic nitrogen compounds (such as ammonia and pyridine). These support the notion that the surface of MCM-41 bears higher acid site strength than amorphous silica.

The acidity of the surface is shown to drop with the level of loadings as evidenced by the reduction of the fluorescence lifetime of NA\*. This may be due to the reduction of the overall acidity as the first NA interacts with the silanol groups of the highest acid strengths. It is also possible that the polarity within the channel and the

solvation effect change with loading especially if there was a close proximity between the silanol sites, or it may be that adsorbates-adsorbate interaction become appreciable at high loadings.

MCM-41 with narrower pore diameter ( $d_p = 36.6 \text{ \AA}$ ; synthesised using microwave heating) was reported [4] to have a higher catalytic activity for the cracking of polyethylene than the MCM-41 with larger pore diameter ( $d_p = 50.9 \text{ \AA}$ ; synthesised using convention oven). Although the technique reported in this paper showed the two materials to be acidic and to protonate NA, it was unable to detect a difference between the acidity of the two materials.

Finally, one of the outstanding issues in zeolite science is the question whether silicalite-1 has intrinsic catalytic activity or the presence of amphoteric metal impurities was the source of this activity. It might be argued accordingly that the presence of acid sites on the surface of all-silica MCM-41 was due to similar impurities. All that can be said on this is that we have taken care in making sure the vessels used in the synthesis of these materials were free as much as possible from impurities. PTFE lined autoclaves were used and cleaned internally using hydrofluoric acid. The source of silica used was Ludox-AS40, which is one of the purest sources of silica. Furthermore, chemical analysis of the MCM-41 samples showed that aluminium impurity was below 10 ppm level, which is the limit of the analytical instrument if one takes into account the practical limit for fusing and diluting a large amount of the sample.

### 3. Conclusions

The polarity within the channel environment of all-silica MCM-41 and the surface acidity were probed by the adsorption of RhB and NA, respectively. The photochemical properties of these probe compounds were studied by laser-induced fluorescence spectroscopy and compared with their properties in liquid solutions. The channel's environment was found to be polar and similar to the polarity present in methanol solution. The lactone form of RhB-L was present in non-polar solvents having dielectric constant ( $\epsilon \leq 15$ ), whereas in polar solvents ( $\epsilon > 15$ ), the solutions were red in colour indicating the opening of the lactone ring and the formation of the RhB-Z form in the ground state. When adsorbed within MCM-41 pores, RhB-L transformed into the RhB-Z form or even was protonated to the RhB-C. Both the fluorescence wavelength  $\lambda_{\text{max}}$  and the fluorescence decay rate of the excited state confirmed the presence of the opening of the lactone ring within the MCM-41 channels. It was not possible to ascertain whether the RhB-Z form had been protonated to form RhB-C because of lack of distinction between the presence of the two forms.

It has been shown, however, that NA was protonated by the surface of MCM-41 at the ground state as confirmed by the excitation spectra. The proton was given back to the surface of the solid when the adsorbed complex was excited with laser. From the  $pK_a$  of the conjugate acid of NA and the fluorescence decay time of the neutral form it was estimated that the acidity of the surface was equivalent to a perchloric acid aqueous solution with pH 1.8–2.5, depending on the loading level of the NA on MCM-41. The origin of the acidity of the all-silica MCM-41 was concluded to be the silanol groups known to be present on the surface of the channels and there would be a distribution of acid site strength depending on the silanol group environment. It was also concluded that the polarity in the channel and the solvating effect of the surface should have an influence on the acidity of the surface. The results were in agreement with previous findings showing the surface of the all-silica MCM-41 to be catalytically active for the cracking of polyethylene.

### Acknowledgment

We would like to acknowledge the financial support for this research by King Abdulaziz City for Science and Technology (KACST); and the Department of Chemistry of King Fahd University of Petroleum and Minerals (KFUPM) for their general support. We also appreciate the opportunity given by Dr. H. Al-Masoudi from the Center for Applied Physical Sciences (CAPS), Research Institute to use the laser facility.

### References

- [1] S. Biz and M.L. Occelli, *Catal. Rev. Sci. Eng.* 40 (1998) 329.
- [2] A. Corma, *Chem. Rev.* 97 (1997) 2373.
- [3] E.W. Hansen, F. Courivaud, A. Carlson, S. Kolboe and M. Stocker, *Microporous Mesoporous Mater.* 22 (1997) 309.
- [4] Z.S. Seddegi, U. Budrthumal, A.A. Al-Arfaj, A.M. Al-Amer and S.A.I. Barri, *Appl. Catal. A* 225 (2002) 167.
- [5] V. Ramamurthy, *J. Am. Chem. Soc.* 116 (1994) 1345.
- [6] J.C. Scaiano, N.C. De Locas, J. Andraos and H. Garcia, *Chem. Phys. Lett.* 233 (1995) 5.
- [7] B.H. Milosavljevic and J.K. Thomas, *J. Phys. Chem.* 92 (1988) 2997.
- [8] P. Hite, R. Krasnansky and J.K. Thomas, *J. Phys. Chem.* 90 (1986) 5295.
- [9] X. Liu, K.K. Iu and J.K. Thomas, *J. Phys. Chem.* 93 (1989) 4120.
- [10] J.K. Thomas, *Chem. Rev.* 93 (1993) 301.
- [11] X. Liu, K.K. Iu and J.K. Thomas, *J. Phys. Chem.* 98 (1994) 7877.
- [12] S.A. Rutten and J.K. Thomas, *J. Phys. Chem. B* 102 (1998) 598.
- [13] S. Corrent, P. Hahn, G. Pohlers, T.G. Connolly, G.C. Scaiano, and H. Garcia, *J. Phys. Chem. B* 102 (1998) 5852.
- [14] S.A. Rutten and J.K. Thomas, *J. Phys. Chem. B* 103 (1999) 1278.
- [15] M. Alvaro, H. Garcia, S. Corrent and J.C. Scaiano, *J. Phys. Chem. B* 102 (1998) 7530.
- [16] N. Negishi, M. Fujino, H. Yamashita, M.A. Fox and M. Anpo, *Langmuir* 10 (1994) 1772.
- [17] U.K.A. Klein and F.W. Hafner, *Chem. Phys. Lett.* 43 (1976) 246.

- [18] J.L. Dela Cruz and G.J. Blanchard, J. Phys. Chem. A 106 (2002) 10718.
- [19] M. Barra, J.J. Cosa and R.H. de Rossi, J. Org. Chem. 55 (1990) 5850.
- [20] J. Karpiuk, Z.R. Grabowski and F.C. De Schryver, Proc. Indian Acad. Sci. 104 (1992) 133.
- [21] R. Krasnansky and J.K. Thomas, in *The Colloidal Chemistry of Silica*, H.E. Bergna (ed) (1994) 223.
- [22] C.P. Tripp and M.L. Hair, Langmuir 12 (1996) 3952.
- [23] J.H. Anderson, J. Lombardi and M.L. Hair, J. Colloid Interface Sci. 50(3) (1975) 519.
- [24] M.L. Hair and W. Herl, J. Phys. Chem. 73 (1969) 4269.
- [25] A.A. El-Rayyes, H.P. Perzanowski, U.K.A. Klein, and S.A.I. Barri, Cata. Lett. 78 (2002) 161.
- [26] A.A. El-Rayyes, H.P. Perzanowski, S.A.I. Barri and U.K.A. Klein, J. Phys. Chem. A. 105 (2001) 10169.
- [27] P.A. Jalil, M.A. Al-Daous, A.A. Al-Arfaj and A.M. Al-Amer, J. Beltramini S.A.I. Barri, Appl. Catal. A 207 (2001) 159.